

Synthesis, structure, and thermochemistry of adduct formation between N-heterocyclic carbenes and isocyanates or mesitylnitrile oxide

Manuel Temprado · Subhojit Majumdar ·
Xiaochen Cai · Burjor Captain · Carl D. Hoff

Received: 20 June 2013 / Accepted: 27 June 2013
© Springer Science+Business Media New York 2013

Abstract Reaction of N-heterocyclic carbenes (NHCs) with isocyanates yields stable zwitterionic imidates/amidates in toluene solution. These compounds were fully characterized and the crystal structures of several species were determined by X-ray crystallography. The thermochemistry of binding of these and related species was studied by solution calorimetry. Comparison is made of the enthalpies of binding of NHC to isocyanates (RNCO) and isomeric nitrile oxides (RCNO) as well as CO₂. DFT calculations were performed to additionally assess the nature of bonding in these compounds.

Keywords Carbenes · NHC · Zwitterions · Betaines · Thermochemistry

Introduction

The isolation and characterization of the first stable crystalline carbene was performed by Arduengo et al. [1]. Since then, these species have generated great interest in several different

fields of chemistry due to their important applications as ligands in organometallic complexes [2–6], and as organic catalysts [7–11]. By far, the most used carbenes nowadays are N-heterocyclic carbenes (NHCs) derived from imidazole. The stability of NHCs arises from a combination of electronic effects, π -donation by the lone pairs of the N atoms into the empty p_{π} orbital of the carbene, and steric effects incorporating bulky substituents in the nitrogens. NHCs are strong σ -donors and their application as powerful nucleophilic reagents has been documented in several important organic catalyzed transformations [7–15]. It is well known that addition of NHCs to electrophilic reagents leads to formation of zwitterionic adducts [16–18]. In this regard, Louie and co-workers have synthesized and structurally characterized a series of zwitterionic imidazolium carboxylates by reaction of NHCs with CO₂ [19, 20]. Analogously, the synthesis and X-ray structures of a series of imidazol(in)ium dithiocarboxylates [21] and thio-carboxylates [22] have also been reported by Delaude et al. We have recently reported [23] that addition of solid MesCNO (Mes = mesityl) to a toluene solution of NHC resulted in the immediate formation of the corresponding NHC/MesCNO adduct. Moreover, Severin and co-workers [24] have also reported characterization of stable covalent adducts of NHCs with N₂O. Likewise, isothiocyanate adducts of NHC are also known [16–18]. Furthermore, NHCs have been reported as catalysts for the trimerization of isocyanates to form the corresponding isocyanurates in THF solution [14]. Until recently, it was accepted in the literature that addition of isocyanates to NHCs does not usually stop at the zwitterionic stage. Delaude stated that isolation of the adducts was proven impossible, even at low temperatures in the presence of an excess of NHCs [18]. The only structural data for binding of an isocyanate to an NHC the authors could find was the report of Schmidt et al. [25] where an indazoliumamidate obtained by trapping of the corresponding NHC with an isocyanate was structurally

Special Issue in honor of Prof. Maria Victoria Roux.

Electronic supplementary material The online version of this article (doi:10.1007/s11224-013-0305-2) contains supplementary material, which is available to authorized users.

M. Temprado (✉)
Department of Physical Chemistry, Universidad de Alcalá, Ctra.
Madrid-Barcelona Km. 33,600, 28871 Madrid, Spain
e-mail: manuel.temprado@uah.es

S. Majumdar · X. Cai · B. Captain · C. D. Hoff (✉)
Department of Chemistry, University of Miami, 1301 Memorial
Drive, Coral Gables, FL 33146, USA
e-mail: c.hoff@miami.edu

characterized and the recent report of Ong and co-workers [26] where the structure of an amine-linked NHC which binds isocyanates at both the NHC and amine functionality is determined. However, the authors have not been able to find reports of the structure of simple adducts between NHCs and isocyanates. Surprisingly, we were able to isolate and characterize the pale yellow RNCO adducts of IPr, SIPr, and IMes (R = PhNCO, *p*-F₃CC₆H₄NCO, Adamantyl; IPr = 1,3-bis(diisopropyl)phenylimidazol-2-ylidene, SIPr = 1,3-bis(diisopropyl)phenylimidazolin-2-ylidene, IMes = 1,3-bis(mesityl)imidazol-2-ylidene; Fig. 1) by addition of stoichiometric amounts of solid RNCO to a toluene solution of the corresponding NHC. These adducts presumably correspond to the active species in the catalyzed trimerization [10], but they can be isolated in toluene solution in the absence of excess PhNCO, a finding not previously reported in spite of their use as catalysts [14]. This work reports the isolation and characterization of stable adducts of NHC and isocyanates in toluene solution and the comparison of the structure and thermochemistry of their formation with the corresponding MesCNO adducts recently reported by us [23]. In addition, thermochemical studies of NHC adducts of CO₂ [19, 20] are made for comparative purposes.

Experimental

General considerations

Unless stated otherwise, all operations were performed in a Vacuum Atmospheres dry box under an atmosphere of purified argon. Toluene was dried and deoxygenated by distillation from sodium benzophenone ketyl under argon into flame dried glassware. Deuterated solvents were purchased from Aldrich and stored over molecular sieves 4 Å in the glove box. NHCs were purchased from Strem Chemical and used as-received. Mesityl nitrile oxide (MesCNO)¹ and SIPr/MesCNO [23] were prepared and recrystallized according to the literature. ¹H NMR spectra were recorded on a Bruker Avance 400 MHz spectrometer at room temperature. ¹H NMR chemical shifts are reported in parts per million (ppm) with respect to the protio impurities referenced at 7.16 ppm for C₆D₆ and 2.09 ppm for toluene-*d*⁸. FTIR spectra were obtained using a Perkin Elmer Spectrum 400 FTIR Spectrometer in CaF₂ solution cells obtained from Harrick Scientific or for solids on a Perkin Elmer Universal ATR Sampling Accessory. Mass spectra were run on a Bruker BioFlex IV MalDI-TOF Mass Spectrometer. Calorimetric

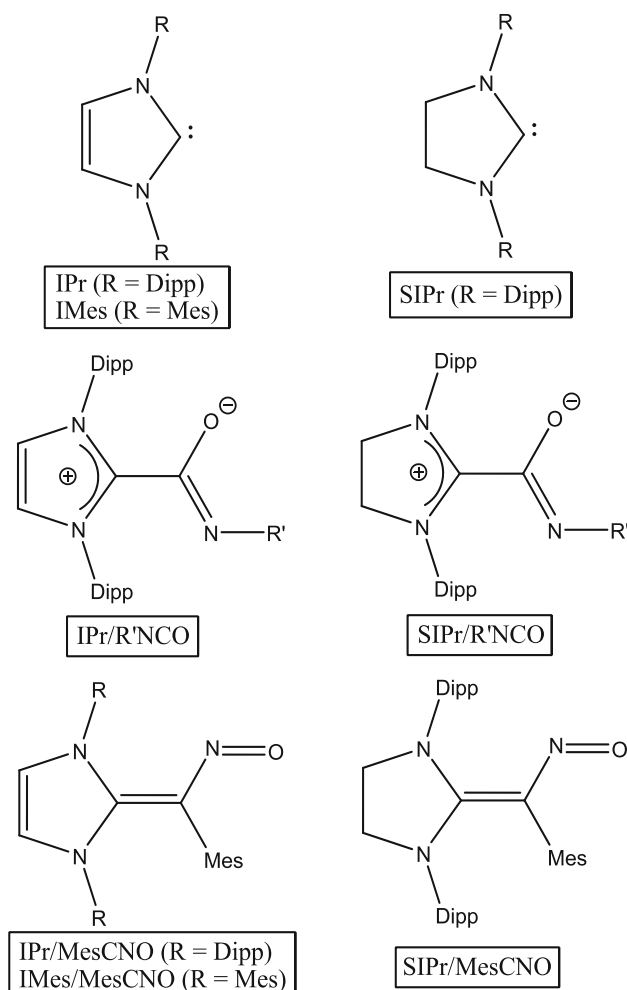


Fig. 1 Structures of carbenes and adducts (Dipp = 2,6-diisopropylphenyl, Mes = mesityl, R' = Ph, *p*-F₃CC₆H₄, Adamantyl)

measurements were made using a Setaram C-80 Calvet microcalorimeter.

Preparation of the NHC/MesCNO and NHC/RNCO adducts

In the glove box, 0.1657 g of solid MesCNO (1.03 mmol, 1 eq) was added to a solution of 0.400 g IPr (1.03 mmol, 1 eq) in 10 mL toluene and the mixture was shaken to dissolve the MesCNO. The solution turned red-orange and some solid began to precipitate out. It was left undisturbed in the glove box overnight. Evaporation of toluene led to isolation of the pure red-orange adduct in near quantitative yield. Similar procedures were used for other adducts. Adducts were fully characterized by ¹H NMR, IR, UV-vis, MS, and in some cases X-ray structure determination. In the case of IPr/MesCNO, elemental analysis was also performed. NMR data, Mass Spec., and NMR data for all the complexes are summarized below. Structural data are reported in a later section.

¹ For a description see supporting information files in Ref. [27] which presents a modified preparation from the original (Ref. [28]).

IPr/PhNCO

The light yellow adduct showed a strong peak in the Maldi-TOF at $m/z = 508.34$ corresponding to MH^+ (for $C_{34}H_{41}N_3O$ m/z (calc) = 507.32). 1H NMR (400 MHz, C_6D_6): $\delta = 7.66$ (d, 2H, *o*-Ph of PhNCO), 7.20 (t, 2H, *p*-Ar of IPr), 7.13 (m, 2H, *m*-Ph of PhNCO), 7.06 (d, 4H, *m*-Ar of IPr), 6.79 (t, 1H, *p*-Ph of PhNCO), 6.14 (s, 2H, vinylic H of IPr), 2.70 (septet, 4H, CH of iPr), 1.38 (d, 12H, CH_3 of iPr), 1.08 (d, 12H, CH_3 of iPr) ppm. IR: of the solid: 3164, 3136, 3097, 3074, 2962, 2930, 2870, 1708, 1613, 1581, 1557, 1476, 1446, 1385, 1362, 1333, 1310(sh), 1230, 1239(sh), 1207, 1182, 1089(sh), 1062, 1022 cm^{-1} .

SIPr/PhNCO and SIPr/F₃CC₆H₄NCO

The light yellow adduct showed a strong peak in the Maldi-TOF at $m/z = 510.35$ corresponding to MH^+ (for $C_{34}H_{43}N_3O$ m/z (calc) = 509.34). 1H NMR (400 MHz, C_6D_6): $\delta = 7.62$ (d, 2H, *o*-Ph of PhNCO), 7.09 (t, 2H, *p*-Ar of SIPr), 6.99 (d, 4H, *m*-Ar of SIPr), 6.80 (m, 2H, *m*-Ph of PhNCO), 6.75 (t, 1H, *p*-Ph of PhNCO), 3.38 (s, 4H, CH_2 of SIPr), 3.28 (septet, 4H, CH of iPr), 1.55 (d, 12H, CH_3 of iPr), 1.19 (d, 12H, CH_3 of iPr) ppm. IR: of the solid: 2964, 2929, 2868, 1702, 1662, 1621, 1596, 1586, 1547, 1499, 1481, 1464, 1447, 1384, 1309, 1281, 1259, 1085(sh), 1052, 1021 cm^{-1} .

For SIPr/ $F_3CC_6H_4NCO$ analogous procedures were followed as for SIPr/PhNCO, and it was characterized for comparative purposes based solely on its crystal structure reported in a later section and detailed in SI.

IPr/AdNCO

The light yellow adduct showed a strong peak in the Maldi-TOF at $m/z = 566.41$ corresponding to MH^+ (for $C_{38}H_{51}N_3O$ m/z (calc) = 565.40). 1H NMR (400 MHz, C_6D_6): $\delta = 7.21$ (t, 2H, *p*-Ar of IPr), 7.09 (d, 4H, *m*-Ar of IPr), 6.11 (s, 2H, vinylic H of IPr), 2.81 (septet, 4H, CH of iPr), 1.75 and 1.62 (d, 6H, CH_2 in AdNCO), 1.52 (d, 12H, CH_3 of iPr), 1.09 (d, 12H, CH_3 of iPr) ppm.

IPr/MesCNO

The red adduct showed a strong peak in the Maldi-TOF at $m/z = 550.38$ corresponding to MH^+ (for $C_{37}H_{47}N_3O$ m/z (calc) = 549.37). 1H NMR (400 MHz, C_6D_6): $\delta = 7.08$ (t, 2H, *p*-Ar of IPr), 6.93 (d, 4H, *m*-Ar of IPr), 6.51 (s, 2H, *m*-Ar of MesCNO), 6.22 (s, 2H, vinylic H of IPr), 3.02 (septet, 4H, CH of iPr), 2.07 (s, 3H, *p*- CH_3 of MesCNO), 1.97 (s, 6H, *o*- CH_3 of MesCNO), 1.23 (d, 12H, CH_3 of iPr), 1.02 (d, 12H, CH_3 of iPr) ppm. IR: 3168, 2964, 2930, 2870, 1567, 1495, 1464, 1456, 1446, 1428(sh), 1385, 1361, 1328, 1235, 1221, 1203, 1182(sh), 1173,

1150, 1121, 1079, 1061, 1037 cm^{-1} . UV-vis (toluene, 20 °C): $\lambda_{max} = 563$ nm. Anal. Calcd. for $C_{37}H_{47}N_3O$: C, 80.83; H, 8.62; N, 7.64. Found: C, 79.48; H, 8.50; N, 7.01.

IMes/MesCNO

The red adduct showed a strong peak in the Maldi-TOF at $m/z = 438.3$ corresponding to MH^+ (for $C_{29}H_{31}N_3O$ m/z (calc) = 437.25). 1H NMR (400 MHz, C_6D_6): $\delta = 6.53$ (d, 4H, *m*-Ar of IMes), 6.42 (s, 2H, *m*-Ar of MesCNO), 5.72 (s, 2H, vinylic H of IMes), 2.08 (s, 3H, *p*- CH_3 of MesCNO), 2.03 (s, 18H, *o*- CH_3 of IMes, *o*- CH_3 of MesCNO), 1.98 (s, 6H, *p*- CH_3 of IMes) ppm. IR: 2912.1, 1610.6, 1505.3, 1447.1, 1330.6, 1284.3, 1229.3(sh) cm^{-1} .

Solution calorimetric measurements

A representative experimental procedure is described; for other data see Table 1. In the glove box a solution of 0.0294 g SIPr (0.0756 mmol) was dissolved in 2 mL C_6D_6 and loaded in the outer mixing chamber of the Calvet solution cell. A solution of 0.0190 g SIPr (0.1179 mmol) was dissolved in 2 mL C_6D_6 and loaded in the inner mixing chamber of the Calvet solution cell. The calorimeter cell was sealed, taken from the glove box, and loaded into the Setaram C-80 calorimeter. Following temperature equilibration, the reaction was initiated and the calorimeter rotated to achieve mixing. Following return to baseline the calorimeter cell was taken into the glove box, opened and 1 mL of the solution loaded into an NMR tube which confirmed complete conversion of SIPr (limiting reagent) to the SIPr/MesCNO complex. The heat of this reaction was computed by integration of the thermogram and yielded $\Delta H = -29.0$ kcal/mol. The reaction was repeated four times to give a final average value of $\Delta H = -29.9 \pm 1.3$ kcal/mol. In some cases SIPr was used as the limiting reagent, and in some cases MesCNO was used as the limiting reagent and the values were the same within experimental error.

Displacement of AdNCO from SIPr/AdNCO by CO_2

In the glove box a 1/1 mol ratio solution was prepared containing 10 mg AdNCO and 22 mg SIPr in 2 mL of C_6D_6 . To two NMR tubes fitted with rubber septa, 1 mL of this solution was added, the tubes sealed and taken from the glove box. To one of the tubes 4 mL CO_2 (gas) was added utilizing a Hamilton gas tight syringe. After approximately 3 min, a white precipitate of SIPr/ CO_2 appeared in this tube. An NMR spectrum was run confirming disappearance of the peaks due to SIPr/AdNCO and appearance of weak bands due to the sparingly soluble SIPr/ CO_2 and strong bands due to free AdNCO at 1.68,

Table 1 Selected computed geometrical parameters and enthalpies of binding

Adduct	C–C ^a (Å)	Torsional angle ^b (°)	ΔH_{calc} (kcal/mol) ^c	ΔH_{expt} (kcal/mol)
IPr/MesCNO	1.445, 1.415 ^c	27, 30 ^c	–29.3	–27.0 ± 0.6
SIPr/MesCNO	1.420 ^d , 1.399 ^c 1.487 ^c	26 ^d , 25 ^c 89 ^c	–32.8 –12.9	–29.9 ± 1.3
IPr/PhNCO	1.521 ^c	90 ^c	–18.8	–25.1 ± 0.4
SIPr/PhNCO	1.521, 1.528 ^c 1.522 ^c	90, 90 ^c 52 ^c	–19.1 –18.1	–22.6 ± 0.8
IPr/CO ₂	1.510 ^e	89 ^e		–19.7 ± 2.5 ^f
SIPr/CO ₂	1.535 ^e	59 ^e		–17.3 ± 2.5 ^f
IPr/AdNCO	1.524	50		–13.4 ± 0.4
SIPr/AdNCO				–14.5 ± 0.4

^a C–C distance linking the NHC to RCNO, RNCO or CO₂. Unless stated otherwise, bond distances were obtained by X-ray crystallography.

^b Dihedral angle between the NCN (NHC) and XYZ (NCO for RNCO, CCN for RCNO and OCO for CO₂) planes. Unless stated otherwise dihedral angles were obtained by X-ray crystallography. ^c Calculated values at the M05-2X/6-311G(d,p) level; for the SIPr/MesCNO and SIPr/PhNCO systems two minima were computed, see text for additional discussion. ^d Value obtained from Ref. [23]. ^e Value obtained from Ref. [20]. ^f Based on enthalpy of substitution by PhNCO of the NHC/CO₂ adduct in CH₂Cl₂ solution as described in text. Due to the differing solvent conditions, an estimated uncertainty of ±2.5 kcal/mol is assigned

1.56, and 1.28 ppm as confirmed by direct comparison to an authentic sample.

Attempted displacement of CO₂ from SIPr/CO₂ by AdNCO

In the glove box, 10 mg SIPr/CO₂ and 4.6 mg AdNCO (≈ 1/1 molar ratio) were dissolved in 0.7 mL CDCl₃ and transferred to an NMR tube which was sealed and taken out of the glove box. The NMR spectrum showed the starting materials SIPr/CO₂ and AdNCO and no new peaks grew in. The solution remained colorless and conversion to SIPr/AdNCO was not observed.

Displacement of CO₂ from SIPr/CO₂ by PhNCO

In the glove box, approximately 20 mg SIPr/CO₂ was added to an NMR tube. To this was added 1.5 equivalents of PhNCO dissolved in 1 mL C₆D₆. This resulted in formation of a white slurry which slowly dissolved with evolution of gas bubbles. After approximately 30 min an NMR spectrum was run and showed quantitative conversion to SIPr/PhNCO whose preparation is described above.

Crystallographic analyses

Each crystal was glued onto the end of a thin glass fiber. X-ray intensity data were measured by using a Bruker SMART APEX2 CCD-based diffractometer using Mo K α radiation ($\lambda = 0.71073$ Å) [29]. The raw data frames were integrated with the SAINT+ program by using a narrow-

frame integration algorithm [29]. Corrections for Lorentz and polarization effects were also applied with SAINT+. An empirical absorption correction based on the multiple measurement of equivalent reflections was applied using the program SADABS. All structures were solved by a combination of direct methods and difference Fourier syntheses, and refined by full-matrix least-squares on F², by using the SHELXTL software package [30, 31]. Crystal data, data collection parameters, and results of the analyses are listed in Table S1.

Colorless single crystals of SIPr/PhNCO suitable for X-ray diffraction analyses obtained by evaporation of solutions of toluene 25 °C, crystallized in the orthorhombic crystal system. The systematic absences in the intensity data were consistent with either space group *Pnma* or space group *Pna2*₁. The former space group was chosen initially for structure solution tests. This space group was confirmed by the successful solution and refinement of the structure. With *Z* = 4, the molecule has crystallographic mirror symmetry.

Colorless single crystals of SIPr/*p*-F₃CC₆H₄NCO suitable for X-ray diffraction analyses obtained by evaporation of solvent from toluene at 25 °C, crystallized in the orthorhombic crystal system. The systematic absences in the intensity data indicated two possible space groups, *Pnm2*₁ or *Pmnn*. The structure could only be solved in the former space group. With *Z* = 2, the molecule has crystallographic mirror symmetry. The CF₃ group is disordered over two orientations and was refined in the ratio 50:50.

Colorless single crystals of IPr/AdNCO suitable for X-ray diffraction analyses obtained by evaporation of

solvent from a benzene solution at 25 °C, crystallized in the monoclinic crystal system. The systematic absences in the intensity data were consistent with the unique space group $P2_1/c$. One molecule of benzene cocrystallized with the complex and is present in the asymmetric crystal unit.

Red single crystals of IPr/MesCNO suitable for X-ray diffraction analyses were obtained by slow evaporation of benzene. The systematic absences in the intensity data were consistent with the unique space group $P2_1/n$. All non-hydrogen atoms were refined with anisotropic displacement parameters. Hydrogen atoms were placed in geometrically idealized positions and included as standard riding atoms during the least-squares refinements. Half a molecule of benzene, and one water molecule cocrystallized with the complex and is present in the asymmetric crystal unit. The presence of water presumably occurs from advantageous water slowly condensing into the system during the long time needed to grow crystals. Reasonable peak positions for the H atoms on the water molecules were located in the difference map and then refined with geometric restraints.

Yellow single crystals of IMes/MesCNO suitable for X-ray diffraction analyses obtained by evaporation of solutions of toluene at 25 °C, crystallized in the monoclinic crystal system. The systematic absences in the intensity data were consistent with the unique space group $P2_1/n$. One water molecule cocrystallized with the complex and is present in the asymmetric crystal unit. The presence of water presumably occurs from advantageous water slowly condensing into the system during the long time needed to grow crystals. Reasonable peak positions for the H atoms on the water molecules were located in the difference map and then refined with geometric restraints.

Computational details

Electronic structure calculations were carried out using the M05-2X [32] density functional with the 6-311G(d,p) basis set as implemented in the Gaussian 09 suite of programs [33]. Minima optimizations were performed by computing analytical energy gradients. The obtained stationary points were characterized by performing energy second derivatives, confirming them as minima by the absence of negative eigenvalues of the Hessian matrix of the energy. Computed electronic energies were corrected for zero-point energy, and thermal energy to obtain the corresponding H^0 values. To derive binding energies, the basis set superposition error (BSSE) was computed using counterpoise calculations [34, 35]. Finally, time-dependent (TD) DFT calculations were carried out to compute the electronic transition for all molecules.

Results

Synthetic and structural studies

All NHCs studied (Scheme 1) were found to react rapidly and cleanly at room temperature in toluene solution with isocyanates to produce the corresponding NHC/RNCO adducts as confirmed by NMR spectroscopy. ^1H NMR spectra show that these adducts are stable for more than 2 days at room temperature in toluene solution. This behavior is in contrast to that observed in THF solution in which case the catalytic trimerization of isocyanates to form the corresponding isocyanurates is observed [14].

Suitable crystals for X-ray analysis of SIPr/PhNCO, SIPr/*p*-F₃CC₆H₄NCO, IPr/AdNCO (Ad = adamantyl), IPr/MesCNO, and IMes/MesCNO were grown by dissolving crude samples of the adducts in toluene or benzene, followed by slow evaporation of the solutions in an open vial at room temperature in the glove box. The solid state structure of adducts SIPr/PhNCO, IPr/AdNCO, and IPr/MesCNO are shown in Figs. 2, 3, and 4, respectively. The structures of SIPr/*p*-F₃CC₆H₄NCO and IMes/MesCNO, as well as full crystallographic data are available in the Supplemental Material. The crystal structure of SIPr/MesCNO has been previously reported [23].

During crystal growth of IPr/MesCNO, and IMes/MesCNO, adventitious H₂O slowly entered and was present in the unit cell. It is not known how this lattice water affects the primary structure of the adduct. There is a similarity in the bond distances and angles for the two new structures to the previously reported SIPr/MesCNO which did not contain water in the unit cell. This is reflected in the C–C distance linking the NHC to MesCNO and also the dihedral angle between the NHC NCN plane and the CCN plane of MesCNO where the distances and angles are: SIPr/MesCNO (1.42 Å, 26.1°); IPr/MesCNO·H₂O·1/2CH₆ (1.45 Å, 26.5°); IMes/MesCNO·H₂O (1.45 Å, 24.2°). The dihedral angle and the C–C distance in the structures is $25.4^\circ \pm 1.2^\circ$ and 1.44 ± 0.02 Å, respectively, for the three structures in spite of the inclusion of water in the unit cell of two of the three structures. These values are also similar to the ones reported recently by Bielawski and co-workers [36] for several NHC adducts of 2,6-dimethoxybenzotrile N-oxide.

Louie and co-workers [20] have shown that for NHC adducts of CO₂ a wide range of dihedral angles are observed in the crystal structure and that the torsional angle was dependent upon the steric bulk of the N-substituent in the imidazolium ring. Thus while the CO₂ adduct of IPr had an angle of $\approx 90^\circ$ that of IMe was $\approx 29^\circ$. A correlation was found in thermogravimetric analysis (TGA) between the decarboxylation temperature and the torsion angle which decreased with increasing torsional angle. While the

Scheme 1 Possible resonance structures for NHC adducts of MesCNO (*top*) and RNCO (*bottom*). For both isomers, a zwitterionic structure can be formulated. For MesCNO formation of an N=O bond allows a stable resonance structure with a C=C bond as in the Wanzlich equilibrium

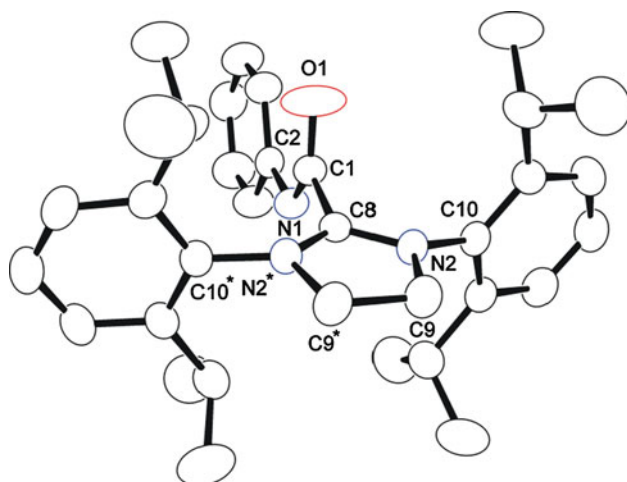
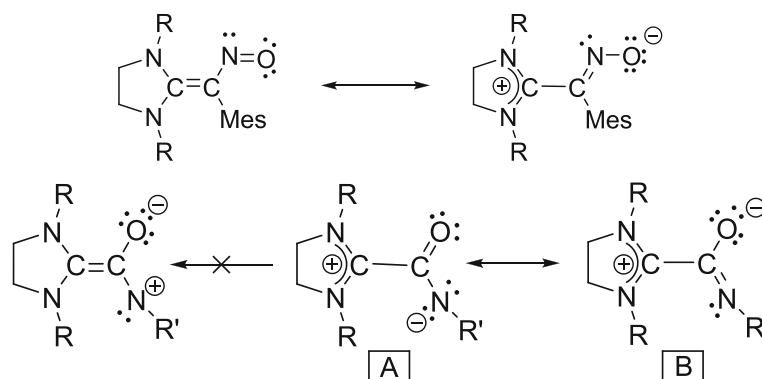


Fig. 2 Thermal ellipsoid plot (40 % probability) of SIPr/PhNCO. Selected distances (Å) and angles (°): C1–C8 = 1.521(4), C8–N2 = 1.326(2), C10–N2 = 1.451(2), C1–O1 = 1.242(3), C1–N1 = 1.282(3), C1–C8–N2 = 123.88(11), C1–C8–N2* = 123.88(11), N2*–C8–N2 = 111.5(2). The angle between the N1–C1–O1 plane and the N2–C8–N2* plane = 90.0°

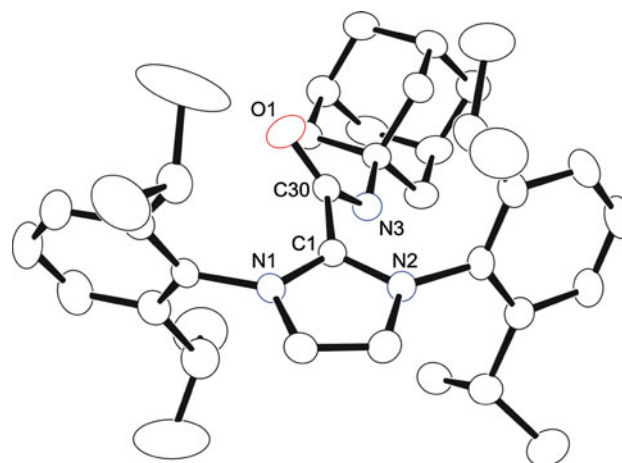


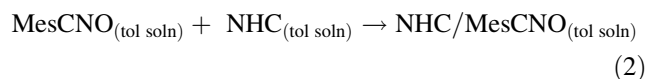
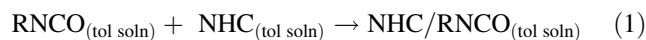
Fig. 3 An ORTEP showing the molecular structure of IPr/AdNCO, with thermal ellipsoids set at 30 % probability. Selected distances (Å) and angles (°): C1–C30 = 1.524(4), C30–O1 = 1.247(4), C30–N3 = 1.293(4), C1–N1 = 1.342(4), C30–C1–N1 = 127.3(3), C30–C1–N2 = 126.2(2), N1–C1–N2 = 106.4(3). The angle between the N3–C30–O1 plane and the N1–C1–N2 plane = 49.5°

most common reported structure of NHC betaines appears to be one in which the NHC and the other moiety are perpendicular to each other, that may reflect in part that X-ray quality crystals may be more easily obtained in the orthogonal configuration and thus for those complexes for which structures can be determined, it is more common to succeed in obtaining crystals with a 90° torsional angle. The computational studies reported here (see below) appear to show little energy dependence upon the torsional angle in which the central C atom is bound to the NHC as observed here for SIPr/PhNCO (Fig. 2) and SIPr/*p*-F₃CC₆H₄NCO (see Supplementary Material) which displayed a symmetry plane and were crystallographically exactly perpendicular. That was not the case, however, for the IPr/AdNCO adduct in which a dihedral angle between the NCN (NHC) and NCO (RNCO) planes is 49.5°. Moreover, the C–C distance linking the NHC to all isocyanates studied of 1.52 Å is significantly longer than that

found in the MesCNO adducts. A summary of these structural parameters is shown in Table 1.

Solution calorimetric studies

The enthalpies of binding between the IPr or SIPr and MesCNO, PhNCO, or AdNCO in toluene solution were measured by solution calorimetry. The values derived are collected in Table 1. Data for formation of the PhNCO and MesCNO adducts are based on the enthalpy of reaction as measured with all species in toluene solution for formation of the adducts as shown in Eq. 1 for PhNCO and MesCNO in Eq. 2.



For comparative purposes we have measured the enthalpy of reaction of the IPr/CO₂ and SIPr/CO₂ with

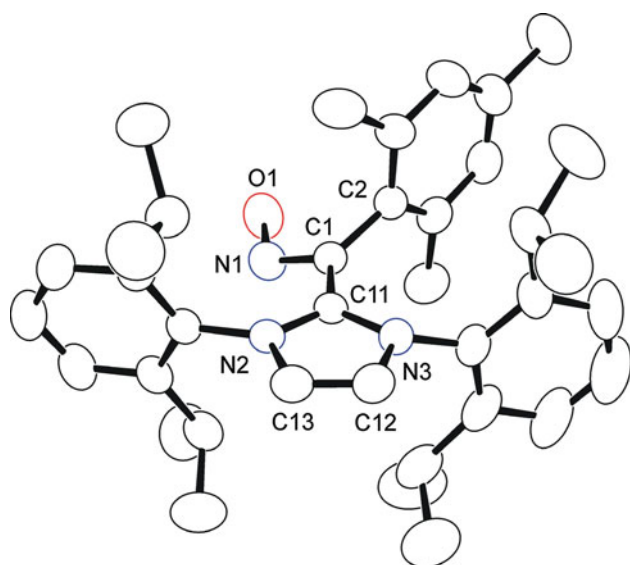
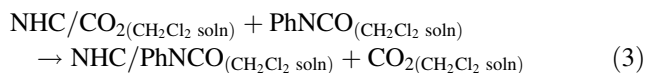


Fig. 4 An ORTEP showing the molecular structure of IPr/MesCNO, with thermal ellipsoids set at 40 % probability. Selected distances (Å) and angles (°): C1–C11 = 1.445(4), N2–C11 = 1.353(3), N1–C1 = 1.323(3), O1–N1 = 1.295(3), C1–C2 = 1.494(4), N2–C11–C1 = 127.5(2), N3–C11–C1 = 126.5(2), N2–C11–N3 = 106.0(2). The angle between the N1–C1–C2 plane and the N2–C11–N3 plane = 26.5°

PhNCO to form the IPr/PhNCO or SIPr/PhNCO adduct. Due to low solubility of the NHC/CO₂ adducts in toluene it was not possible to measure the enthalpy of reaction in this solvent. However, in CH₂Cl₂ it was found that reaction 3 occurred rapidly and cleanly at 30 °C.



$$\Delta H_{\text{IPr}} = -5.4 \pm 0.2 \text{ kcal/mol}$$

$$\Delta H_{\text{SIPr}} = -5.3 \pm 0.3 \text{ kcal/mol}$$

Data for the CO₂ adducts must be viewed with some caution due to the more polar nature of CH₂Cl₂ versus toluene as a solvent. However, for Eq. 3 solvation energies may to some extent cancel for the polar adducts. For both IPr and SIPr the CO₂ adducts are ≈ 5.3 kcal/mol less stable than the PhNCO adducts.

Thermochemical data for reaction of AdNCO with NHC (see Eq. 1) which is 11.7 and 8.1 kcal/mol less exothermic for IPr and SIPr, respectively, than the corresponding reaction of NHC with PhNCO lead to the prediction that while RNCO can replace CO₂ in these adducts when R = Ph (reaction 3), that situation should be reversed for R = Ad and CO₂ should replace the isocyanate in this case as shown in reaction 4.



This prediction was confirmed experimentally in that addition of CO₂ to a toluene solution of IPr/AdNCO

resulted in precipitation of the sparingly soluble IPr/CO₂ carboxylate and formation of free AdNCO as confirmed by NMR spectroscopy. As a further check, addition of AdNCO to a CDCl₃ solution of SIPr/CO₂ resulted in no reaction—in contrast to the displacement that occurs readily as shown in Eq. 3 where PhNCO is capable of displacing CO₂ from its NHC adduct. Thus the binding of CO₂ is intermediate between PhNCO and AdNCO in terms of enthalpy of formation.

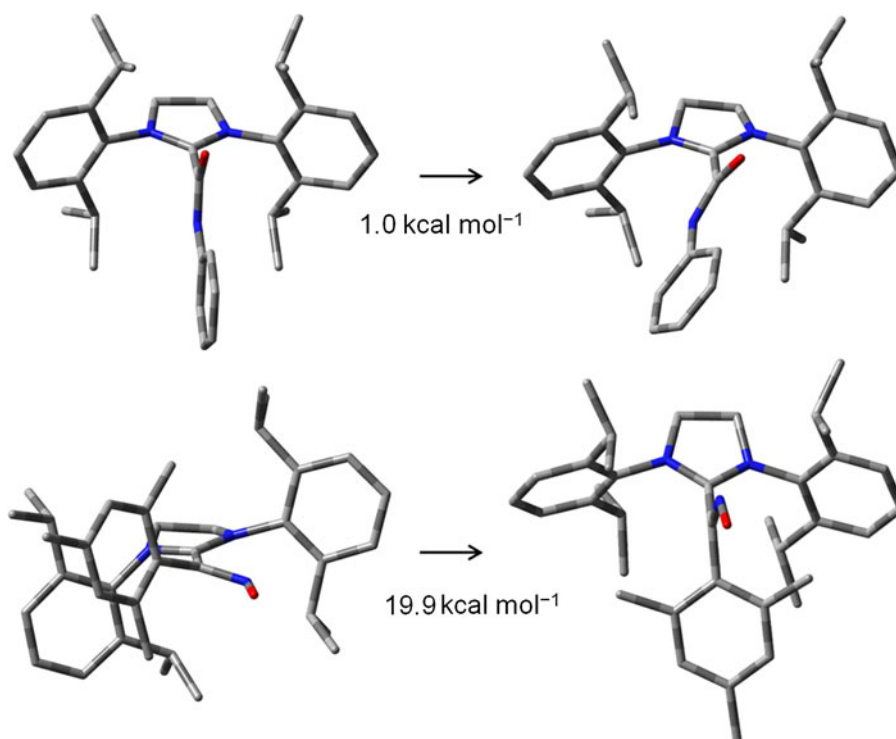
Computational studies

In order to further analyze the structural and energetic differences observed in these adducts, DFT computational studies were undertaken. The first question addressed was the reason for the structural differences observed between the MesCNO and RNCO adducts. As shown in Fig. 5, the computed structures at the M05-2X/6-311G(d,p) level for PhNCO perpendicular to the plane of the SIPr ring and for MesCNO approaching coplanarity are computed to be the most stable in agreement to the solid state structures determined by X-ray crystallography of both adducts. In the case of PhNCO, two different minima with a N–C–N dihedral angle between the NHC and isocyanate moieties of 90.0° or 52.4° were located with only a 1.0 kcal/mol difference between the two conformations. The structure of the minimum with a dihedral angle of 52.4° is similar to that obtained for the IPr/AdNCO adduct in this work by X-ray crystallography (49.5°). In contrast, for MesCNO, the difference between the two structures with an almost perpendicular arrangement and the one approaching coplanarity is nearly 20 kcal/mol. In fact, the orthogonal structure shown in Fig. 5 corresponds to a transition state connecting two equivalent minima with a dihedral angle of 25°.

An additional indication of π-bonding in the MesCNO adducts is their color. The dramatic differences in color between the adducts are also of interest, in particular the fact that monomeric nitroso compounds are often blue in color [37]. Reasonably good computation of the UV–vis spectra of these adducts could be obtained at the TD-M05-2X/6-311G(d,p) level of theory. Experimental and computed data are: SIPr/MesCNO: λ_{max}(exp) = 605 nm; λ_{max}(calc) = 714 nm; IPr/MesCNO: λ_{max}(exp) = 563 nm; λ_{max}(calc) = 640 nm. For IPr/PhNCO and SIPr/PhNCO no absorptions in the visible region were located. Although calculations overestimate the value of λ_{max}, they predict qualitatively the shift in the adducts.

IR data also provide additional insight in the nature of the adducts. The IR of monomeric nitroso compounds often displays ν_{NO} near 1,550 cm⁻¹ whereas dimeric nitroso compounds which have a similar structure to the zwitterionic resonance structures shown in Scheme 1 for SIPr/

Fig. 5 Computed structures and energies of conformational change for selected conformations of adducts SIPr/PhNCO (*top*) and SIPr/MesCNO (*bottom*)



MesCNO show a band near $1,250\text{ cm}^{-1}$ [37]. The IR spectrum of IPr/MesCNO displays a band at $1,567\text{ cm}^{-1}$. When compared to frequency calculations performed at the M05-2X/6-311G(d,p) level, this frequency can be assigned as being predominantly an NO stretch though it is coupled to other modes of vibration.

Discussion

One goal of this work was to evaluate the relative stability of the NHC adducts we recently reported for nitrile oxides (RCNO) [23] with their isomeric isocyanate counterparts (RNCO). Assuming that the NHC will coordinate to the C atom preferentially, this gives two different bonding topologies. For RCNO (isoelectronic with CO_2), the bond formed between the NHC and the C atom will be at the central atom, whereas for RNCO, the bond will be at a terminal site of the XYO moiety (For RCNO; X = C, Y = N; For RNCO: X = N, Y = C). As shown in Scheme 1 for MesCNO, two structural formulations can be made in simple bonding theory—a zwitterionic form as well as one involving a C=C bond in a Wanzlich equilibrium-type structure [38–40].

The simple analysis in Scheme 1 shows that bonding to the central atom as in PhNCO and CO_2 will yield primarily a zwitterionic formulation of the adduct, whereas for MesCNO where the bonding C is in a terminal position an additional driving force is provided by potential formation

of a C=C bond provided an approximately coplanar structure can be achieved. In SIPr/PhNCO, the plane containing PhNCO is perpendicular to the plane of the NHC implying no π -bonding interaction between the $\text{C}_{\text{carbene}}$ and PhNCO since the relevant p orbitals are orthogonal. The zwitterionic structure would have free rotation about the C–C bond and to reduce steric repulsion would be expected to adopt the orthogonal structure displayed. While in the solid state, the C–C distances between the NHC and the isocyanate fragments of the PhNCO and AdNCO adducts are comparable, the dihedral angles between both moieties are markedly different for the PhNCO (90° , Fig. 2) and the AdNCO (49.5° , Fig. 3). A dihedral angle of 59.0° between the imidazolium and the carboxylate groups has been previously observed for the SIPr/ CO_2 adduct [20].

Due to the fact that the zwitterionic formulation in RNCO is further stabilized by amidate (species A in Scheme 1)/imidate (species B in Scheme 1) resonance structures, it seems likely that for the ionic structure binding to the central rather than a terminal atom might have an advantage due to this added stability. Furthermore, a through-space attractive attraction between the electronic deficient carbenoid carbon and the electron rich O and N atoms (Scheme 1) would confer an additional stability to the RNCO adducts [22, 41].

The situation with MesCNO is less clear since the dihedral angle between the imidazolium and the nitrile oxide fragment in the adducts is $25.4^\circ \pm 1.2^\circ$. The torsional angle is controlled by steric and electronic effects as

well as crystal packing forces. The importance of electronic effects is clear since CO_2 , which is smaller than MesCNO, nevertheless has a larger dihedral angle. It seems likely that steric factors prevent the MesCNO adducts from adopting a planar structure. Nonetheless, partial π bonding between the carbenoid C of the NHC and the C atom of MesCNO might be indicated. In fact, the C–C bond length of $1.44 \pm 0.02 \text{ \AA}$ for the MesCNO adducts supports more double bond character than for the isocyanate adducts (C–C = 1.52 \AA) in agreement with a more favorable delocalization of the π -electronic cloud in the more planar compounds. Computational studies also confirm the existence of π -bonding in the MesCNO adducts where a difference of nearly 20 kcal/mol is computed between the two structures shown in Fig. 5 as the plane of the NHC is rotated away from that of the MesCNO plane. In contrast, for PhNCO the two conformers shown in Fig. 5 differ only by 1 kcal/mol. Additional evidence of the different nature in both kind of adducts is their color, whereas nitrile oxide adducts exhibit high intensity bands in the visible spectra the isocyanate adducts are pale yellow. The presence of a band at $1,567 \text{ cm}^{-1}$ assigned to a NO stretch in the typical range for nitroso compounds in the IR spectrum of IPr/MesCNO also support the formulation of these species as nitrosoethylene compounds (resonance structure on the left for the SIPr/MesCNO adduct in Scheme 1).

While differences occur in the apparent preference for IPr versus SIPr in the adducts, these are close to the overlap of experimental error and at this time detailed discussion of them is not warranted. Additional studies may allow further refinement, but at this time we are assigning an average value for the enthalpy of binding of IPr and SIPr to the adducts and note that the enthalpies of binding (kcal/mol) are in order: MesCNO (-28.5 ± 1.5) > PhNCO (-23.9 ± 1.3) > CO_2 (-18.5 ± 1.2) > AdNCO (-14.0 ± 0.6).

The position of the CO_2 adduct as being intermediate between PhNCO and AdNCO is confirmed in that displacement of CO_2 by PhNCO is spontaneous as shown in Eq. 3, but displacement of AdNCO by CO_2 is spontaneous as shown in Eq. 4. The greater stability of the PhNCO adduct compared to the CO_2 adduct is in keeping with the fact that the NHC/ CO_2 adduct can be used as an isocyanate oligomerization catalyst precursor [14] since the CO_2 is readily displaced by ArNCO. The average value reported here for PhNCO (-23.9) is surprisingly close to that derived for binding of PhNCS to IMes by Bielawski and co-workers [42] of -23 kcal/mol.

The ≈ 10 kcal/mol difference in stability of the PhNCO and AdNCO adducts is striking and is attributed to both steric and electronic effects. The more electron withdrawing nature of Ph compared to Ad group will increase the positive charge on the C atom of RNCO and increase the favorability of forming the zwitterionic structure.

Moreover, in the PhNCO case, the negative charge in the zwitterionic structure can be delocalized into the phenyl ring since the PhNCO moiety is planar (see Figs. 2, 5). In addition, as stated previously, the dihedral angle between the NHC and the isocyanate moieties is markedly different for the PhNCO (90°) and AdNCO (49.5°) adducts. Therefore, the former can benefit from a through-space attractive interaction as discussed previously more markedly than the latter. Furthermore, it should be expected that the steric hindrance imposed by the bulky substituents in the imidazoli(in)um nitrogens destabilize the adduct more pronouncedly for the bulkier AdNCO as compared to PhNCO.

Conclusions

This work reports the synthesis, isolation, and characterization of stable isocyanate adducts of IPr and SIPr. The X-ray structures of zwitterionic adducts of these commercial NHC with isocyanates are reported here for the first time. This has been proven possible due to the enhanced stability of the adducts in toluene solution as opposed to that in THF, a solvent in which the trimerization of isocyanates to form the corresponding isocyanurates in presence of NHC was observed [14] indicating the essential role that the polar solvent plays in this catalytic transformation.

Addition of IPr or SIPr to PhNCO or MesCNO give two different kind of adducts which can be described as zwitterions (PhNCO) or conjugated neutral species (MesCNO). Simple bonding pictures as well as detailed computations show that changing the binding site from the center of the conjugated system (ArNCO and OCO) to a terminal site (ArCNO) appears to enhance the role of π bonding between the two C atoms in a Wanzlich-like C=C bond formation. This form is stabilized by concurrent formation of an N=O π bond and the adducts approximate being conjugated nitrosoethylene compounds. In spite of the added source of stability provided by the partial π bonding between the NHC and MesCNO, the ArCNO adducts are only ≈ 5 kcal/mol more stable than the ArNCO adducts and ≈ 10 kcal/mol more stable than the CO_2 adducts. In part this may be due to an increased stability of the zwitterionic formulation of the central bonded adducts due to imidate/amidate resonance stabilization and by further delocalization of the negative charge in the phenyl ring in the case of PhNCO, a factor not possible in the MesCNO adducts since the mesityl and the CNO moieties are almost perpendicular (see Figs. 4, 5). Moreover, a through-space attractive electrostatic interaction between the electronic deficient carbenoid carbon and the electron rich N and O atoms of the RNCO moiety may also confer additional stability to the zwitterionic isocyanate adducts, partially

compensating for the loss of C=C bonding. Further studies on related species are in progress to better understand the nature of these adducts and to further explore their reactivity.

Acknowledgments Support of this work by the National Science Foundation Grant CHE 0615743 (C. D. H.) and by the Spanish Ministry of Economy and Competitiveness (MINECO) under CTQ2012-36966 (M. T.) is gratefully acknowledged. The authors thank Professor Janis Louie at the University of Utah for helpful discussions.

References

- Arduengo AJ III, Harlow RL, Kline M (1991) *J Am Chem Soc* 113:361
- Herrmann WA, Köcher C (1997) *Angew Chem Int Ed* 36:2162
- Crudden CM, Allen DP (2004) *Coord Chem Rev* 248:2247
- Garison JC, Youngs WJ (2005) *Chem Rev* 105:3978
- Hahn FE, Jahnke MC (2008) *Angew Chem Int Ed* 47:3122
- Díez-González S, Marion N, Nolan SP (2009) *Chem Rev* 109:3612
- Nair V, Bindu S, Sreekumar V (2004) *Angew Chem Int Ed* 43:5130
- Marion N, Díez-González S, Nolan SP (2007) *Angew Chem Int Ed* 46:2988
- Enders D, Niemeier O, Henseler A (2007) *Chem Rev* 107:5606
- Fèvre M, Pinaud J, Gnanou Y, Vignolle J, Taton D (2013) *Chem Soc Rev* 42:2142
- Ryan SJ, Candish L, Lupton DW (2013) *Chem Soc Rev* 42:4906
- Nair V, Rajesh C, Vinod AU, Bindu S, Sreekanth AR, Mathen JS, Balagopal L (2003) *Acc Chem Res* 36:899
- Nair V, Bindu S, Sreekumar V, Rath NP (2003) *Org Lett* 5:665
- Duong HA, Cross MJ, Louie J (2004) *Org Lett* 6:4679
- Nair V, Sreekumar V, Bindu S, Suresh E (2005) *Org Lett* 7:2297
- Kuhn N, Al-Sheikh A (2005) *Coord Chem Rev* 249:829
- Kirmse W (2005) *Eur J Org Chem* 237
- Delaude L (2009) *Eur J Inorg Chem* 1681
- Duong, HA, Tekavec TN, Arif AM, Louie J (2004) *Chem Commun* 112
- Van Ausdall BR, Glass JL, Wiggins KM, Aarif AM, Louie J (2009) *J Org Chem* 74:7935
- Delaude L, Demonceau A, Wouters J (2009) *Eur J Inorg Chem* 1882
- Hans M, Wouters J, Demonceau A, Delaude L (2011) *Eur J Org Chem* 7083
- Cai X, Majumdar S, Fortman GC, Frutos LM, Temprado M, Clough CR, Cummins CC, Germain ME, Palluccio T, Rybak-Akimova EV, Captain B, Hoff CD (2011) *Inorg Chem* 50:9620
- Tskhovrebov AG, Solari E, Wodrich MD, Scopelliti R, Severin K (2012) *Angew Chem Int Ed* 51:232
- Schmidt A, Habeck T, Lindner AS, Snovydyovych B, Namyslo JC, Adam A, Gjikaj M (2007) *J Org Chem* 72:2236
- Li CY, Kuo YY, Tsai JH, Yap GPA, Ong TG (2011) *Chem Asian J* 6:1520
- Barybin MV, Diaconescu PL, Cummins CC (2001) *Inorg Chem* 40:2892
- Grundmann C, Dean JM (1965) *J Org Chem* 30:2809
- Apex2 Version 2.2-0 and SAINT + Version 7.46A (2007) Bruker Analytical X-ray System, Inc., Madison
- Sheldrick GM (2000) SHELXL Version 6.1. Bruker Analytical X-ray Systems, Inc., Madison
- Sheldrick GM (2008) *Acta Crystallogr A* 64:112
- Zhao Y, Schultz NE, Truhlar DG (2006) *J Chem Theory Comput* 2:364
- Frisch MJ et al (2010) Gaussian 09, revision B.01. Gaussian, Inc., Wallingford, CT
- Simon S, Duran M, Dannenberg JJ (1996) *J Chem Phys* 105:11024
- Boys SF, Bernardi F (1970) *Mol Phys* 19:553
- Lee YG, Moerdyk JP, Bielawski CW (2012) *J Phys Org Chem* 25:1027
- Gowenlock BG, Richter-Addo GB (2004) *Chem Rev* 104:3315
- Taton TA, Chen P (1996) *Angew Chem Int Ed* 35:1011
- Denk, MK, Hezarkhani A, Zheng FL (2007) *Eur J Inorg Chem* 3527
- Poater A, Ragone F, Giudice S, Costabile C, Dorta R, Nolan SP, Cavallo L (2008) *Organometallics* 27:2679
- Nakayama J, Kitahara T, Sugihara Y, Sakamoto A, Ishii A (2000) *J Am Chem Soc* 122:9120
- Norris BC, Sheppard DG, Henkelman G, Bielawski CW (2011) *J Org Chem* 76:301